Published in final edited form as:
J Neurochem. 2012 April ; 121(1): 146–156. doi:10.1111/j.1471-4159.2012.07647.x.

Retinal cone and rod photoreceptor cells exhibit differential susceptibility to light–induced damage

Kiichiro Okano[1], **Akiko Maeda**[1,2], **Yu Chen**[1], **Vishal Chauhan**[2], **Johnny Tang**[2], **Grazyna Palczewska**[3], **Tsutomu Sakai**[4], **Hiroshi Tsuneoka**[4], **Krzysztof Palczewski**[1], and **Tadao Maeda**[1,2,5]

[1]Department of Pharmacology, Case Western Reserve University, Cleveland, 44106, U.S. A

[2]Department of Ophthalmology & Visual Sciences, Case Western Reserve University, Cleveland, 44106, U.S. A

[3]Polgenix, Inc., Cleveland, 44106, U.S. A

[4]Department of Ophthalmology, Jikei University School of Medicine, Tokyo, 105, Japan

Abstract

All-*trans*-retinal and its condensation-products can cause retinal degeneration in a light–dependent manner and contribute to the pathogenesis of human macular diseases such as Stargardt's disease and age–related macular degeneration (AMD). Although these toxic retinoid by–products originate from rod and cone photoreceptor cells, the contribution of each cell type to light–induced retinal degeneration is unknown. Here the primary objective was to learn whether rods or cones are more susceptible to light–induced, all–*trans*–retinal–mediated damage. Previously, we reported that mice lacking enzymes that clear all–*trans*–retinal from the retina, ATP–binding cassette transporter 4 (ABCA4) and retinol dehydrogenase 8 (RDH8), manifested light-induced retinal dystrophy. We first examined early-stage-AMD patients and found retinal degenerative changes in rod-rich rather than cone-rich regions of the macula. We then evaluated transgenic mice with rod–only and cone–like–only retinas in addition to progenies of such mice inbred with *Rdh8*$^{-/-}$ *Abca4*$^{-/-}$ mice. Of all these strains, *Rdh8*$^{-/-}$ *Abca4*$^{-/-}$ mice with a mixed rod–cone population showed the most severe retinal degeneration under regular cyclic light conditions. Intense light exposure induced acute retinal damage in *Rdh8*$^{-/-}$ *Abca4*$^{-/-}$ and rod–only mice but not cone–like–only mice. These findings suggest that progression of retinal degeneration in *Rdh8*$^{-/-}$ *Abca4*$^{-/-}$ mice is affected by differential vulnerability of rods and cones to light.

Keywords

visual cycle; photoreceptor; retinoid; retina; Stargardt's disease; age-related macular degeneration

NTRODUCTION

The number and localization of rods and cones in the retina vary widely among species. A rod–dominant distribution featuring a mosaic pattern of rods and cones with a ratio of 98:2 is observed in nocturnal species such as the mouse (Jeon *et al*. 1998), whereas cones predominate in diurnal species such as the ground squirrel (Mustafi *et al*. 2009). Humans are

[5]Correspondence to: Tadao Maeda, M.D., Ph.D., Department of Ophthalmology & Visual Sciences, School of Medicine, Case Western Reserve University, 2085 Adelbert Road, Room 115, Cleveland, Ohio 44106, USA; Phone: +1-216–368–6103, Fax: +1-216–368–3171, txm88@case.edu.

Conflict of interest statement None.

a diurnal species, but with a rod–dominant retina featuring 92 million rods and 4.6 million cones with an unusual distribution (Curcio *et al*. 1990). Cones are concentrated in the center of human retina, the macula, which comprises only 4% of the retina but is responsible for most human vision (Mustafi *et al*. 2009). The macula is organized into three regions: the fovea, parafovea and perifovea (Fig. 1A). Cones at a high density of about 0.2 million cells/mm^2 are mostly localized in the center of the fovea, a rod–free zone with a diameter of 0.35 mm (1.25° visual angle). The density of cones falls steeply by an order of magnitude at the parafovea 1 mm away from the foveal center where cones are replaced with rods. The number of rods increase markedly at the perifovea with the highest density located in a ring surrounding the fovea at about 4.5 mm (18° visual angle) (Curcio *et al*. 1990). This characteristic distribution of cones and rods in the macula is what provides high–definition vision.

Several forms of retinal degeneration occur specifically in the macula. These include two blinding diseases: Stargardt's disease (STGD) and age−related macular degeneration (AMD). STGD is a juvenile form of macular degeneration that leads to a progressive loss of central visual function, most commonly with an autosomal recessive inheritance pattern (Rotenstreich *et al*. 2003, Molday & Zhang 2010). AMD is a disease of complex etiology with a progression affected by multiple genetic and environmental factors (Klein *et al*. 2004, Coleman *et al*. 2008, Patel *et al*. 2008). Notably, the accumulation of toxic retinoid cycle by–products, including di–retinoid–pyridinium–ethanolamine (A2E), produced by the conjugation of two molecules of all–*trans*–retinal, has been detected in retinas of patients with either STGD or AMD. Therefore, accumulation of retinoid condensation metabolites and/or abnormally high levels of their precursor, all–*trans*–retinal, at least in part, suggest a common etiology for these two macular disorders (Liu *et al*. 2000, Rattner & Nathans 2006, Cideciyan *et al*. 2004, Molday 2007, Shroyer *et al*. 2001, Maeda *et al*. 2011, Tsybovsky *et al*. 2010).

Recently, we reported that mice lacking two enzymes critical for all–*trans*–retinal clearance from rod and cone outer segments, namely ATP–binding cassette transporter 4 (ABCA4) and retinol dehydrogenase 8 (RDH8), demonstrate retinal degeneration with pathological features similar to human macular degeneration under regular cyclic light and severe photoreceptor cell death after intense light exposure (Maeda *et al*. 2008, Maeda *et al*. 2009a, Maeda *et al*. 2011). This mouse model provides a special opportunity to study anomalies in retinoid metabolism that could contribute to the progression of STGD and AMD.

In this study, we investigated whether rods or cones are more susceptible to light-induced, all-*trans*-retinal-mediated damage. First, retinas of patients with early–stage AMD were examined by spectral–domain optical coherence tomography (SD–OCT) to assess the regional distribution of early *in vivo* pathological changes within the macula. In addition, rod–only, cone–like–only, and both rod and cone mouse models were employed to investigate if rods and cones were differentially susceptible to light-induced retinal degeneration. These transgenic strains with their unique photoreceptor distributions were crossbred with $Rdh8^{-/-}$ $Abca4^{-/-}$ mice to evaluate photoreceptor cell type–dependent progression of all–*trans*–retinal–associated retinal degeneration both under regular cyclic light conditions and after brief exposure to intense light. The overall results indicating greater rod than cone vulnerability to light-induced retinal damage add to our expanding knowledge of photoreceptor degeneration in STGD and AMD.

MATERIALS AND METHODS

Human subjects, retinal fundus, cross–sectional imaging and kinetic visual fields

Patients with early stage AMD (n=6, 2 females and 4 males, 9 eyes; ages 63–83 years) and healthy volunteers (n=17, 7 females and 10 males, 17 eyes; ages 57-84 years) were included in this study. Early AMD was defined by the presence of one or more large (>63 μm) drusen and/or focal hyperpigmentation without choroidal neovascularization or geographic atrophy, and a visual acuity of 20/60 or better (Scilley *et al*. 2002). The study was approved by the Institutional Review Boards/Ethics Committees at Jikei University Hospital and adhered to the tenets of the Declaration of Helsinki. All participants gave written informed consent and underwent a complete ophthalmoscopic examination that included biomicroscopy, color photography, SD–OCT and standard automated perimetry (SAP). SD–OCT images were obtained with Cirrus OCT (Carl Zeiss Meditec, Dublin, CA). Topographical mapping of the macular region was carried out as previously published (Tangelder *et al*. 2008, Curcio *et al*. 1990). SAP was performed with a Humphrey field analyzer 750 (Zeiss–Humphrey, Dublin, CA) according to the standard protocol. The 10–2 program with the Swedish interactive threshold strategy was used to analyze SAP input.

Animals

Cone–DTA Rdh8$^{-/-}$ *Abca4*$^{-/-}$ and *Nrl*$^{-/-}$ *Rdh8*$^{-/-}$ *Abca4*$^{-/-}$ triple knockout mice were generated and genotyped as previously described (Maeda *et al*. 2008). Mice with the leucine residue variant at amino acid position 450 of RPE65 were used for this study and the numbers of female and male mice were the same. Cone–DTA mice and *Nrl*$^{-/-}$ mice were acquired from Dr. Jeremy Nathans (Johns Hopkins University, Baltimore, MD) and Dr. Anand Swaroop (National Eye Institute, Bethesda, MD), respectively. All mice were housed in the animal facility at the School of Medicine, Case Western Reserve University, where they were maintained either under complete darkness or in a 12 h light (~50 lux) /12 h dark cyclic environment. Manipulations in the dark were performed under dim red light transmitted through a Kodak No.1–safelight filter (transmittance > 560 nm). All animal procedures and experiments were approved by the Case Western Reserve University Animal Care Committees and conformed to recommendations of both the American Veterinary Medical Association Panel on Euthanasia and the Association of Research for Vision and Ophthalmology. Primate retina samples were obtained from Ricerca Bioscience LLC (Concord, OH).

Histology and immunohistochemistry

Histological and immunohistochemical procedures were carried out as previously described (Maeda *et al*. 2005). Iimmunohistochemical images were viewed with a Zeiss LSM 510 inverted Laser Scan Confocal Microscope. 4, 6–diamidino–2–phenylindole (DAPI) and Alexa 488–conjugated peanut agglutinin (PNA) were purchased from Invitrogen. 1D4 (anti–rhodopsin mouse monoclonal antibody) was a gift from Dr. Robert Molday (University of British Columbia, Vancouver, Canada).

Induction of light–induced retinal damage in mice

Light-induced retinal degeneration was induced in 6-week-old mice as previously described (Maeda *et al*. 2009a).

Ultra–high resolution spectral–domain optical coherence tomography (SD–OCT) and scanning laser ophthalmoscopy (SLO) imaging

Both ultra–high resolution SD–OCT (Bioptigen, Research Triangle, NC) and SLO (HRAII, Heidelberg Engineering, Heidelberg, Germany) were employed as previously described (Shiose *et al*. 2011).

Electroretinograms (ERGs)

All ERG procedures were performed using previously published methods (Maeda *et al*. 2005).

Retinoids and A2E analyses

All experimental procedures related to extraction, derivatization, and separation of retinoids from dissected mouse eyes were carried out as described before (Maeda *et al*. 2005).

Statistical analyses

Experimental results were analyzed by the one way ANOVA–test with p values of < 0.05 considered statistically significant.

RESULTS

Early retinal changes in patients with AMD indicate parafoveal rod loss

To assess the initial lesions of AMD *in vivo*, retinal cross–sectional images were obtained by high–definition SD–OCT from patients with early–stage AMD. Irregular alignment of the outer nuclear layer (ONL) was frequently observed (8/9 eyes) in the non–foveal macular region (parafovea and/or perifovea) whereas the structure and thickness of the ONL at the central fovea was well maintained (Fig. 1A and Table 1). Standard automated perimetry (SAP) was performed as well in these patients to evaluate sensitivity changes in the macular region (68 data points within a 10° visual field) by two parameters, namely mean deviation (MD; mean difference of sensitivity to light–targets with various luminance and sizes between tested and ‘normal’ expected visual sensitivity) and pattern standard deviation (PSD; a measurement of the degree to which the shape of a patient’s measured visual field departs from the ‘normal’ age–corrected reference field model). Both MD and PSD for tested AMD patients were in the normal range except for one eye and visual acuity was maintained as well (Table 1). The discrepancy between structural damage documented by SD–OCT versus the preserved visual function estimated by visual field and acuity examinations probably resulted because the sensitivity of SAP was not sufficient to reveal pathological changes in the parafoveal region clearly detected by SD–OCT.

Cones and rods form a heterogeneous mosaic pattern in the macular regions of both humans and primates (Mustafi *et al*. 2009). To illustrate the distribution of cones and rods in this region, the central part of primate (adult cynomolgus monkey) retina was examined (Fig. 1B). The fovea was highly populated with cones (regions a and b) with a density in the center (region a) 20% higher than in region b, 0.12 mm away. In both regions c (parafovea; 2.0 mm away from the foveal center) and d (perifovea; 4.5 mm away from the center), the population of rods was significantly higher than cones. Finally, the density of rods in region d was about 20% higher than in region c. These observations are consistent with the results of primate retina immunohistochemistry in our previous study (Jacobson *et al*. 2007) and similar findings have been reported in primates and humans (Curcio *et al*. 1990, Curcio *et al*. 1987). These observations suggest that the initial retinal changes in AMD may occur in the rod-rich parafoveal and perifoveal regions where cones and rods coexist. Moreover, even though most external light projects to the foveal region of the macula with a high population

of cones, the morphology of the fovea is not initially affected in AMD. Taken together with the SD-OCT findings, the most obvious speculation is that human cones are intrinsically more resistant than rods to degeneration, presumably due to light exposure. Whether cone distribution or the cone/rod ratio plays an additional role in such retinal degeneration is still unknown.

Light-induced retinal damage in mice generated with rod–only, cone–like–only or both rod and cone retinas

To investigate the toxic effects of light exposure on rod and cone photoreceptor cells, we employed mouse models with rod–only, cone–like–only, and both rod and cone retinas. Mice with rod–only retinas were bred by inserting a cone–specific diphtheria toxin A transgene (referred to as cone–DTA) which eliminates cones from the retina (Soucy *et al*. 1998). And the neural retina leucine zipper (Nrl)–deficient mouse was used as a cone–like–only model because this mouse expresses only cone–like cells due to lack of the transcription factor Nrl (essential for rod differentiation and indicated by $Nrl^{-/-}$) (Mears *et al*. 2001). Both strains have been used for cone– and rod–specific characterization (Mears *et al*. 2001, Daniele *et al*. 2005, Kunchithapautham *et al*. 2009, Feathers *et al*. 2008, Chen & Nathans 2007). Wild type (WT) mice with backgrounds matching those of the experimental strains were used as models for retinas with both rods and cones.

Retinas of these different mice at 6 weeks and 4 months of age maintained under a 12 h light (~ 50 lux)/12 h dark cycle were examined functionally, morphologically and biochemically to determine their phenotypic characteristics. Retinal morphology was compared with retinal cross–sectional images and the distribution of photoreceptor cells was evaluated by immunohistochemical (IHC) staining with rhodopsin antibody (1D4) and the cone–sheath specific marker, peanut agglutinin (PNA). In cone–DTA mice at 6 weeks of age, retinal morphology was comparable with that of WT mice (Fig. S1A upper left and upper middle). Rod outer segments were detected whereas cones were largely absent (Fig. S1A lower middle), but both rods and cones were present in WT retina (Fig. S1A lower left). In 6–week–old $Nrl^{-/-}$ mice, rosette formation was observed in regions of the outer retina as previously reported (Daniele *et al*. 2005, Mears *et al*. 2001). The lengths of outer segments were shorter than those visualized in WT and cone–DTA mice (Fig. S1A upper right). In IHC images of retinas from 6–week–old $Nrl^{-/-}$ mice, only cone outer segments were detected by PNA staining and no specific 1D4 signals were observed (Fig. S1A lower right). Photoreceptor populations also were evaluated in DAPI-stained images by measuring the ONL thickness every 400 μm from optic nerve head (ONH) in both superior and inferior retina. The ONL thickness in cone–DTA mice was comparable to that of WT mice at 6 weeks of age. Retinal regions without rosette formation were carefully chosen for ONL thickness measurements in $Nrl^{-/-}$ mice (Fig. S1A right) and their ONL thickness was about 20% less than that of WT mice (Fig. S1B). Retinal function in these different mice at 6 weeks of age was evaluated by single–flash electroretinogram recordings (ERGs). Scotopic-ERG responses in cone–DTA mice were comparable to those of WT mice, whereas $Nrl^{-/-}$ mice showed lower sensitivity to linearly increased light stimuli compared to WT mice (Fig. S1C left panel for each strain; Fig. S1D left). Under photopic conditions, ERG responses were obtained from WT and $Nrl^{-/-}$ mice (enhanced due to higher number of cone-like cells), but these were virtually absent in cone–DTA mice (Fig. S1C right panel for each strain; Fig. S1D right). When retinoid content in the eye was examined by normal phase HPLC, the amount of 11–*cis*–retinal in cone–DTA mice was similar to that in WT mice, whereas the amount in $Nrl^{-/-}$ mice was only 12% of that in WT mice (Fig. S1E). These findings agree with what was expected from the size of the outer segments and the population of photoreceptor cells in each mouse model (Mustafi *et al*. 2009). At 4 months of age, rod function and ONL thickness was maintained in cone–DTA and WT mice, and cone

function was unchanged in *Nrl*$^{-/-}$ and WT mice (Fig. 2). Given these observations, *Nrl*$^{-/-}$ and cone–DTA mice displayed characteristics expected for rod–only and cone–like–only retinas.

Differential progression of retinal degeneration in *Rdh8*$^{-/-}$ *Abca4*$^{-/-}$ mice crossbred with rod–only or cone–like–only mice

Cone–DTA and *Nrl*$^{-/-}$ mice were crossbred with *Rdh8*$^{-/-}$ *Abca4*$^{-/-}$ mice to produce models of rod–only (cone–DTA *Rdh8*$^{-/-}$ *Abca4*$^{-/-}$) and cone–like–only (*Nrl*$^{-/-}$ *Rdh8*$^{-/-}$ *Abca4*$^{-/-}$) retinal degeneration. These mice were kept under a 12 h light (~50 lux)/12 h dark cycle and progression of retinal degeneration was evaluated at 6 weeks and 4 months of age by electrophysiological, histological and biochemical methods. At 4 months of age, retinal structure was also assessed by SD–OCT and the photoreceptor population was evaluated by ONL thickness measurements in DAPI-stained-IHC images. At 6 weeks of age, all tested mouse strains failed to show significant morphological and functional changes between the absence or presence of either *Abca4* or *Rdh8* alone. However, severe photoreceptor cell death was observed in retinas of *Rdh8*$^{-/-}$ *Abca4*$^{-/-}$ mice (~35% cell loss) containing both rods and cones (Fig. 2A left and B left) as compared with WT retinas, just as previously reported (Maeda *et al*. 2009a, Maeda *et al*. 2008). Interestingly, much milder degenerative changes were observed in rod–only and cone–like–only mice crossbred with *Rdh8*$^{-/-}$ *Abca4*$^{-/-}$ mice. In 4–month–old cone–DTA *Rdh8*$^{-/-}$ *Abca4*$^{-/-}$ mice, a mild decrease of ONL thickness (~ 20%) was observed in both the superior and inferior retina as compared to cone–DTA retina (Fig. 2A middle and B middle). In 4–month–old *Nrl*$^{-/-}$ *Rdh8*$^{-/-}$ *Abca4*$^{-/-}$ mice, no significant changes in ONL thickness were noted as compared with *Nrl*$^{-/-}$ mice (Fig. 2A right and B right). Retinal function was evaluated by single–flash ERG recordings under scotopic conditions because scotopic-ERG recording is more sensitive and the preferred way to show progression of retinal dysfunction in *Rdh8*$^{-/-}$ *Abca4*$^{-/-}$ mice even though we also noted attenuation of photopic responses in a previous study (Maeda *et al*. 2008). As shown in Supplement Figure 1, no functional responses were obtained from cone-DTA mice under photopic conditions and photopic ERG responses of *Nrl*$^{-/-}$ mice evidenced responses comparable to those under scotopic conditions. Consistent with the morphological findings, the amplitudes of scotopic functional b–waves in cone–DTA *Rdh8*$^{-/-}$ *Abca4*$^{-/-}$ mice were mildly decreased compared with those in cone–DTA mice but no significant difference was observed between *Nrl*$^{-/-}$ *Rdh8*$^{-/-}$ *Abca4*$^{-/-}$ and *Nrl*$^{-/-}$ mice. This contrasted with the significant decrease of amplitude noted in *Rdh8*$^{-/-}$ *Abca4*$^{-/-}$ mice at 4 months of age (Fig. 2C). These observations suggest that rods are more prone than cones to cell death under room lighting conditions and that degenerative changes are exacerbated in retinas that contain both rods and cones.

Intense light exposure causes severe retinal degeneration in rod–only but not in cone-like-only *Rdh8*$^{-/-}$ *Abca4*$^{-/-}$ mice

To evaluate the susceptibility of cones and rods to acute light–induced stress, mice were exposed to intense levels of light. Six–week–old mice were first dark–adapted for 48 h and then exposed to intense light (10,000 lux) for 30 min. After exposure, mice were kept in the dark for 7 days and the severity of retinal degeneration was evaluated by scotopic-ERG recordings together with SD-OCT imaging *in vivo* followed by IHC examination. ERG amplitudes were drastically attenuated in cone–DTA *Rdh8*$^{-/-}$ *Abca4*$^{-/-}$ mice (>60% decrease) relative to cone–DTA mice (Fig. 3A left). In contrast, ERG amplitudes were only mildly affected in *Nrl*$^{-/-}$ *Rdh8*$^{-/-}$ *Abca4*$^{-/-}$ mice (~15% reduction at higher stimuli: 0 and 12.5 log cd s/m^2) relative to *Nrl*$^{-/-}$ mice (Fig. 3A right). Retinal cross sectional images by SD–OCT *in vivo* and subsequent IHC revealed severe photoreceptor cell death in cone–DTA *Rdh8*$^{-/-}$ *Abca4*$^{-/-}$ mice in which only one or two layers of nuclei remained in the ONL (Fig. 3B), whereas no significant changes in ONL thickness were observed in *Nrl*$^{-/-}$

Rdh8$^{-/-}$ *Abca4*$^{-/-}$ and *Nrl*$^{-/-}$ mice. However, more rosettes were observed in triple knockout mice than *Nrl*$^{-/-}$ mice (Fig. 3C). Of note, *Nrl*$^{-/-}$ *Rdh8*$^{-/-}$ *Abca4*$^{-/-}$ and *Nrl*$^{-/-}$ mice also tolerated 1 h of intense light exposure as well (Fig. S2). We previously reported that accumulation of toxic all–*trans*–retinal after bright light exposure triggers massive light–induced retinal damage in *Rdh8*$^{-/-}$ *Abca4*$^{-/-}$ mice (Maeda *et al*. 2011). Cone–DTA *Rdh8*$^{-/-}$ *Abca4*$^{-/-}$ mice showed a 3–fold higher accumulation of all–*trans*–retinal than cone–DTA mice after intense light exposure (Fig. S3), a level comparable to that of *Rdh8*$^{-/-}$ *Abca4*$^{-/-}$ mice noted previously to exhibit acute retinal degeneration (Maeda *et al*. 2009a, Maeda *et al*. 2008). In contrast, only mild accumulation of all–*trans*–retinal was found in *Nrl*$^{-/-}$ *Rdh8*$^{-/-}$ *Abca4*$^{-/-}$ mice (less than 5% compared with cone–DTA *Rdh8*$^{-/-}$ *Abca4*$^{-/-}$ mice) which also exhibited far less retinal degeneration (Fig. S3). Collectively, these data suggest that rods are more susceptible to intense light–induced damage than cones in *Rdh8*$^{-/-}$ *Abca4*$^{-/-}$ mice.

Fundus autofluorescence (AF) *in vivo* and A2E quantification in rod–only and cone–like–only mouse models

A2E is a major fluorophore component of lipofuscin granules in retinal pigmented epithelial (RPE) cells. Moreover, accumulation of A2E is considered to contribute to the pathogenesis of several types of human macular degeneration, such as AMD and STGD, as well as to retinal degeneration in *Rdh8*$^{-/-}$ *Abca4*$^{-/-}$ mice (Mata *et al*. 2000, Maeda et al. 2008, Murdaugh *et al*. 2010). Autofluorescence (AF) can be detected *in vivo* by ophthalmic scanning laser ophthalmoscopy (SLO) wherein the intensity of the emitted signal is correlated with the level of A2E (Schmitz-Valckenberg *et al*. 2008, Palczewski 2011). SLO is used clinically to investigate the relationship between AF and the progression of retinal degeneration. However, the correlation between increased AF and disease progression in both human and animal models is still controversial (Schmitz-Valckenberg *et al*. 2009b, Schmitz-Valckenberg *et al*. 2009a).

We quantified AF in the fundus and A2E in the above mouse models to examine if photoreceptor cell type affects the accumulation of A2E, and if A2E levels in turn modify the severity of retinal degeneration. SLO examination was carried out with cone–DTA *Rdh8*$^{-/-}$ *Abca4*$^{-/-}$ mice and *Nrl*$^{-/-}$ *Rdh8*$^{-/-}$ *Abca4*$^{-/-}$ mice maintained under a 12 h light (~50 lux)/12 h dark cycle. The intensity of AF from mouse fundus was quantified by calculating mean gray values in mice at 6 weeks, 4 months and 6 months of age whereas amounts of A2E in the eyes were analyzed by reverse phase HPLC at 4 and 6 months of age. At 6 weeks of age, background levels of fluorescence were detectable but there was no significant difference in AF levels in cone–DTA and WT mice caused by deletion of the *Rdh8* and *Abca4* genes (Fig. S4A upper left and upper middle and B). However, AF levels were significantly increased in 6–month–old cone–DTA *Rdh8*$^{-/-}$ *Abca4*$^{-/-}$ and *Rdh8*$^{-/-}$ *Abca4*$^{-/-}$ mouse fundus compared to those in 6–week–old animals, but these changes were much milder in cone–DTA and WT mice (Fig. S4A, lower left and lower middle, and B). Granular spots with weak fluorescence were detected in both 6–week–old and 6–month–old *Nrl*$^{-/-}$ and *Nrl*$^{-/-}$ *Rdh8*$^{-/-}$ *Abca4*$^{-/-}$ mice, and a mild increase of AF intensity was observed with increasing age (Fig. S4A right and B). This observation is consistent with aberrant phagocytosis and transport of A2E to the RPE by these mice (Mustafi *et al*. 2011). However, amounts of A2E in the eye were significantly increased at 4 and 6 months of age in mice lacking *Abca4* and *Rdh8*. More than a 3–fold increase of A2E was noted in *Nrl*$^{-/-}$ *Rdh8*$^{-/-}$ *Abca4*$^{-/-}$ mice than in *Nrl*$^{-/-}$ mice, and a 5–fold elevation was found in cone–DTA *Rdh8*$^{-/-}$ *Abca4*$^{-/-}$ mice compared to cone–DTA mice (Fig. S4C) that correlated with the age–dependent increase of AF in SLO images. These data indicate that all–*trans*–retinal accumulation due to delayed clearance in rods was the dominant source of age–related A2E

accumulation and that the contribution of cones was relatively minor in retinas of *Rdh8*$^{-/-}$ *Abca4*$^{-/-}$ mice.

DISCUSSUION

The primary objective of this study was to investigate whether rods or cones are more susceptible to light-induced, all-*trans*-retinal-mediated damage, an hypothesis recently proposed to explain photoreceptor degeneration during the progression of STGD and AMD (Maeda *et al*. 2011). First, we investigated this question in patients with early–stage AMD, and then focused on genetically altered mouse models.

Recent advances in *in vivo* imaging technology such as SD–OCT and SLO enabled us to obtain high–resolution images from the retinas of human patients (Schmitz-Valckenberg *et al*. 2008, Fleckenstein *et al*. 2008). The highest density of rods in the retina is located in an ellipsoid ring of 3–5 mm eccentricity in the parafovea and we found these rods most severely affected. Previous anatomical analyses of a human eye by Curcio and colleagues revealed that 30% of rods are lost in the parafoveal region of a normal aging eye, and that this loss is accentuated in early–stage AMD eyes by an additional 30–40% (Curcio *et al*. 1993). Our imaging of human eyes by SD–OCT resulted in the striking observation that a significant decrease of retinal thickness and disruption of the ONL had occurred in the parafoveal and perifoveal (rod-rich) area in more than 50% and 80% of early-stage AMD patients, respectively, whereas the morphology and function of the cone rich central fovea appeared normal in these patients (Fig. 1A and Table 1). From these observations, we speculate that photoreceptors surviving in and around the degenerated lesion in these early AMD retinas were cones rather than rods and these cones were preserved in all of our patients. Cones also are reported more likely to survive in both dry–type and wet–type AMD (Shelley *et al*. 2009, Holz *et al*. 1995). In addition, early–stage AMD patients display a significant impairment of rod–mediated as compared to cone–mediated function consistent with an early decrease of rods relative to cones noted in aging retinas (Curcio et al. 1993, Curcio *et al*. 1996, Owsley *et al*. 2001, Owsley *et al*. 2007). Histological analyses of primate macula revealed that the parafovea, where pathology is frequently found in AMD patients, is a rod–dominant area (Fig. 1B). These observations lead us to hypothesize that rod–dominant areas of the macula are initially impaired in AMD.

Similar changes are also expected in STGD, which is characterized by more rapid retinal degeneration than AMD (Maeda *et al*. 2009b). Reportedly, more than 600 mutations in the *Abca4* gene have been linked to STGD (Allikmets 2007). Although the biological role of ABCA4 and its relevance to retinal degenerative diseases is significant, the structural and functional properties of this transporter remain largely undefined. Lack of ABCA4 could lead to photoreceptor degeneration in STGD, not only because this protein facilitates removal of toxic retinoid products but also because mutant ABCA4 misfolds and mislocalizes, thereby inducing cellular stress (Tsybovsky *et al*. 2010). These hypotheses may also explain why *Abca4*$^{-/-}$ mice display a much milder retinal phenotype than STGD patients with *ABCA4* mutations.

Disabling mutations in genes encoding proteins of the retinoid cycle can cause a spectrum of retinal diseases affecting vision (Thompson & Gal 2003). *Rdh8*$^{-/-}$ *Abca4*$^{-/-}$ mice, especially, display significant degenerative changes in the retina due to accumulation of all–*trans*–retinal, A2E, and other toxic all–*trans*–retinal condensation products (Maeda *et al*. 2008). Both RDH8 and ABCA4 are responsible for the clearance of all–*trans*–retinal produced by the visual (retinoid) cycle required for vision (Maeda *et al*. 2008, Maeda *et al*. 2009a). Under ordinary cyclic lighting conditions, *Rdh8*$^{-/-}$ *Abca4*$^{-/-}$ mice evidenced retinal folds at 6–8 weeks of age followed by severe photoreceptor cell death with hallmarks

characteristic of AMD including lipofuscin accumulation, drusen formation, basal laminar hyaline deposition, RPE cell death and choroidal neovascularization (Maeda *et al*. 2008). Additionally, intense light exposure induces acute photoreceptor cell death in these mice (Shiose et al. 2011, Maeda et al. 2009a). To investigate the contribution of rods and cones to all–*trans*–retinal–mediated retinal degeneration, and examine why the parafoveal region is initially impaired in early AMD, we cross bred rod–only (cone–DTA) and cone–like–only ($Nrl^{-/-}$) mice with $Rdh8^{-/-}$ $Abca4^{-/-}$ mice.

At 4 months of age, only mild to insignificant photoreceptor cell death was observed in cone–DTA $Rdh8^{-/-}$ $Abca4^{-/-}$ and $Nrl^{-/-}$ $Rdh8^{-/-}$ $Abca4^{-/-}$ mice, whereas severe photoreceptor cell death with retinal folds especially in the inferior retina was evident in $Rdh8^{-/-}$ $Abca4^{-/-}$ mice maintained in a normal day/night light cycle (Fig. 2). These observations suggest that retinas with a mixed rod/cone population were more susceptible to degeneration under daily light cyclic conditions. To compare the tolerance of rods and cones to strong light–induced stress, we exposed $Nrl^{-/-}$ $Rdh8^{-/-}$ $Abca4^{-/-}$ mice and cone–DTA $Rdh8^{-/-}$ $Abca4^{-/-}$ mice to intense light sufficient to induce acute retinal damage (Fig. 3). Predictably, cone–DTA $Rdh8^{-/-}$ $Abca4^{-/-}$ mice displayed severe retinal degeneration similar to $Rdh8^{-/-}$ $Abca4^{-/-}$ mice (Maeda *et al*. 2009a, Maeda *et al*. 2008) whereas $Nrl^{-/-}$ $Rdh8^{-/-}$ $Abca4^{-/-}$ mice evidenced much milder changes. Even after 1 h of intense light exposure, severe retinal degeneration was not observed in $Nrl^{-/-}$ $Rdh8^{-/-}$ $Abca4^{-/-}$ mice (Fig. S2). These observations indicate that not only are rods more susceptible to light–induced degeneration, but also that the imbalance of cones and rods caused by initial rod death might induce the characteristic retinal degeneration with fold formation in $Rdh8^{-/-}$ $Abca4^{-/-}$ mice. This speculation is further supported by the finding that retinal fold formation was eliminated by cone–DTA–dependent ablation of cones in a cone–rod dystrophy (CRD) mouse model (*rd/rd* mice) (Chen & Nathans 2007). Indeed, such fold formation does not accompany acute cone cell death observed in Leber congenital amaurosis models such as $Rpe65^{-/-}$ and $Lrat^{-/-}$ mice (Maeda *et al*. 2009b). However, this is not the case for all mouse models of retinal disease. For example, this morphological change was not observed in a mouse model for retinitis pigmentosa (RP), the P23H mutant, caused by rod–cell mediated retinal degeneration (Sakami *et al*. 2011). Additionally, activation of innate immunity was documented in $Rdh8^{-/-}$ $Abca4^{-/-}$ mice (Shiose *et al*. 2011) and other STDG and CRD mouse models similar to that observed in human AMD (Anderson *et al*. 2010, Jones *et al*. 2003), suggesting involvement of an inflammatory component in retinal fold formation. Of note, retinal degeneration was more progressive in the inferior retina than superior retina in $Rdh8^{-/-}$ $Abca4^{-/-}$ mice under daily cyclic lighting conditions (Fig. 2) whereas a broad area of retina was destroyed by intense light exposure (Fig. 3). The mechanism of this progressive pattern still remains unclear. One potential explanation is the characteristic differential distribution of cone pigments in mouse retina. Thus, cone short-wave pigments ($\lambda_{max} \approx 360$ nm) are predominantly expressed in cones of the superior retina whereas mid-wave pigments ($\lambda_{max} \approx 510$ nm) are located in superior retina with an apparent ratio of coexpressed M/S-pigment varying from 1:1 to 1:3,000 that reflects a dorso-ventral retinal gradient (Nikonov *et al*. 2005). The different light sensitivity of cones with S- or M-pigment also could contribute to the difference of susceptibility to light-induced stress. Thus cones with S-pigment tolerate daily light better than those with M-pigment. Importantly, S-pigments are dominantly expressed in cone-like cells of $Nrl^{-/-}$ mice (Mears *et al*. 2001) and cones in the para- and peri-foveal regions of human macula (Mustafi *et al*. 2009). These observations reinforce the proposition that cones are more resistant than rods to light damage and rod-dominant areas of the macula are initially impaired in AMD.

One of the common pathological features of chronic progressive AMD and STGD is the RPE accumulation of A2E, one of the main components of lipofuscin granules (Sparrow 2010). Our research has shown that this accumulation causes an increase in AF. Moreover,

changes in AF and A2E are more obvious in rod–only retinas than in cone–like–only retinas (Fig. S4), most likely due to an over 6–fold accumulation of all–*trans*–retinal in rods after strong light exposure (Fig. S3). Our mouse models manifested an obvious correlation between A2E and AF. Retinal degeneration in cone–DTA $Rdh8^{-/-}Abca4^{-/-}$ mice was much milder than in $Rdh8^{-/-}Abca4^{-/-}$ mice, even though AF and A2E levels were similar (Fig.S4). Inter-cellular interaction between rods and cones could be essential for the development of more severe retinopathy, but this is speculative. Even in the presence of a functional retinoid cycle, A2E, retinal dimer, and other toxic all–*trans*–retinal condensation products can accumulate as a consequence of aging.

In human retina, an increase in AF has been observed in the macula, and more specifically a stronger level of AF has been detected in the rod–dominant parafoveal to perifoveal areas (Schmitz-Valckenberg *et al*. 2009b, Schmitz-Valckenberg *et al*. 2009a). This suggests a strong correlation with our finding that rods accumulated more A2E. The sporadic punctate pattern of AF in human macula could also be caused by environmental factors and age–related changes such as cataracts. The opacity of the lens conferred by a cataract could increase light–scattering, decrease UV filtration and project light onto more light–sensitive macular regions (Michael & Bron 2011). A2E and AF still could be useful biomarkers, however, even though the relationship between AF and the progression of AMD and STGD is still controversial. A2E is not the only cause of AF in the RPE (Schmitz-Valckenberg et al. 2008). Because current SLO methodology for evaluating fundus AF may be inadequate (Palczewska *et al*. 2010), further clinical and animal model studies regarding AF, A2E and disease progression are required to draw conclusions as to whether or not AF is a reliable marker for predicting the prognosis of retinal disease. Advanced retinal imaging systems, including two–photon microscopy, could provide more precise measurements of subcellular biochemical changes that cause AF from toxic retinoid byproducts in the RPE (Palczewska *et al*. 2010) and scanning the morphology of the entire retina including the macula with high–resolution SD–OCT will be required. Information from such studies could be applied to clinical settings wherein early detection of pathological changes can promote development of prophylactic treatments and help prevent progression of retinal dysfunction before visual acuity is adversely affected. Pharmacological interventions with FDA–approved drugs that sequester accumulated all–*trans*–retinal and A2E could be one of many highly effective therapeutic approaches (Maeda *et al*. 2011).

Overall, this study demonstrates that early pathology in AMD occurs in the rod–rich parafoveal and perifoveal regions of human macula. We have shown that the coexistence of cones and rods accelerates retinal degeneration in $Rdh8^{-/-}Abca4^{-/-}$ mice, and that cones and rods have different susceptibilities to light-induced degeneration with a greater accumulation of toxic all–*trans*–retinal occurring in rods. Light–induced rod cell death in the rod–rich parafoveal and perifoveal regions could be one of the most important markers for the initial pathology of human macular degeneration.

Supplementary Material

Refer to Web version on PubMed Central for supplementary material.

Acknowledgments

We thank Drs. L. Webster, H. Fujioka, M. Hitomi, S. Shiose, and K. Ishikawa (Case Western Reserve Univ.) and H. Matsuyama and S. Roos, (Case Western Reserve Univ.) for technical support. This work was supported in part by funding from the National Institutes of Health (K08EY019031, K08EY019880, EY009339, EY 021126, P30 EY11373); a VAMC Career Development Grant; the Research to Prevent Blindness Foundation; Foundation Fighting Blindness; Fight for Sight and the Ohio Lions Eye Research Foundation.

References

Allikmets, R. Retinal Degenerations: Biology, Diagnostics and Therapeutics. Humana Press; Totowa, N.J: 2007. Stargardt disease: from gene discovery to therapy; p. 105-118.

Anderson DH, Radeke MJ, Gallo NB, et al. The pivotal role of the complement system in aging and age-related macular degeneration: hypothesis re-visited. Progress in retinal and eye research. 2010; 29:95–112. [PubMed: 19961953]

Chen J, Nathans J. Genetic ablation of cone photoreceptors eliminates retinal folds in the retinal degeneration 7 (rd7) mouse. Investigative ophthalmology & visual science. 2007; 48:2799–2805. [PubMed: 17525215]

Cideciyan AV, Aleman TS, Swider M, et al. Mutations in ABCA4 result in accumulation of lipofuscin before slowing of the retinoid cycle: a reappraisal of the human disease sequence. Human molecular genetics. 2004; 13:525–534. [PubMed: 14709597]

Coleman HR, Chan CC, Ferris FL 3rd, Chew EY. Age-related macular degeneration. Lancet. 2008; 372:1835–1845. [PubMed: 19027484]

Curcio CA, Medeiros NE, Millican CL. Photoreceptor loss in age-related macular degeneration. Investigative ophthalmology & visual science. 1996; 37:1236–1249. [PubMed: 8641827]

Curcio CA, Millican CL, Allen KA, Kalina RE. Aging of the human photoreceptor mosaic: evidence for selective vulnerability of rods in central retina. Investigative ophthalmology & visual science. 1993; 34:3278–3296. [PubMed: 8225863]

Curcio CA, Sloan KR Jr, Packer O, Hendrickson AE, Kalina RE. Distribution of cones in human and monkey retina: individual variability and radial asymmetry. Science (New York, N Y). 1987; 236:579–582.

Curcio CA, Sloan KR, Kalina RE, Hendrickson AE. Human photoreceptor topography. The Journal of comparative neurology. 1990; 292:497–523. [PubMed: 2324310]

Daniele LL, Lillo C, Lyubarsky AL, Nikonov SS, Philp N, Mears AJ, Swaroop A, Williams DS, Pugh EN Jr. Cone-like morphological, molecular, and electrophysiological features of the photoreceptors of the Nrl knockout mouse. Investigative ophthalmology & visual science. 2005; 46:2156–2167. [PubMed: 15914637]

Feathers KL, Lyubarsky AL, Khan NW, Teofilo K, Swaroop A, Williams DS, Pugh EN Jr, Thompson DA. Nrl-knockout mice deficient in Rpe65 fail to synthesize 11-cis retinal and cone outer segments. Investigative ophthalmology & visual science. 2008; 49:1126–1135. [PubMed: 18326740]

Fleckenstein M, Charbel Issa P, Helb HM, Schmitz-Valckenberg S, Finger RP, Scholl HP, Loeffler KU, Holz FG. High-resolution spectral domain-OCT imaging in geographic atrophy associated with age-related macular degeneration. Investigative ophthalmology & visual science. 2008; 49:4137–4144. [PubMed: 18487363]

Holz FG, Gross-Jendroska M, Eckstein A, Hogg CR, Arden GB, Bird AC. Colour contrast sensitivity in patients with age-related Bruch's membrane changes. German journal of ophthalmology. 1995; 4:336–341. [PubMed: 8751098]

Jacobson SG, Aleman TS, Cideciyan AV, et al. Human cone photoreceptor dependence on RPE65 isomerase. Proceedings of the National Academy of Sciences of the United States of America. 2007; 104:15123–15128. [PubMed: 17848510]

Jeon CJ, Strettoi E, Masland RH. The major cell populations of the mouse retina. The Journal of neuroscience : the official journal of the Society for Neuroscience. 1998; 18:8936–8946. [PubMed: 9786999]

Jones BW, Watt CB, Frederick JM, Baehr W, Chen CK, Levine EM, Milam AH, Lavail MM, Marc RE. Retinal remodeling triggered by photoreceptor degenerations. The Journal of comparative neurology. 2003; 464:1–16. [PubMed: 12866125]

Klein R, Peto T, Bird A, Vannewkirk MR. The epidemiology of age-related macular degeneration. American journal of ophthalmology. 2004; 137:486–495. [PubMed: 15013873]

Kunchithapautham K, Coughlin B, Crouch RK, Rohrer B. Cone outer segment morphology and cone function in the Rpe65-/- Nrl-/- mouse retina are amenable to retinoid replacement. Investigative ophthalmology & visual science. 2009; 50:4858–4864. [PubMed: 19407011]

Liu J, Itagaki Y, Ben-Shabat S, Nakanishi K, Sparrow JR. The biosynthesis of A2E, a fluorophore of aging retina, involves the formation of the precursor, A2-PE, in the photoreceptor outer segment membrane. The Journal of biological chemistry. 2000; 275:29354–29360. [PubMed: 10887199]

Maeda A, Golczak M, Chen Y, et al. Primary amines protect against retinal degeneration in mouse models of retinopathies. Nature Chem Biol. 2011 in press.

Maeda A, Maeda T, Golczak M, Chou S, Desai A, Hoppel CL, Matsuyama S, Palczewski K. Involvement of all-trans-retinal in acute light-induced retinopathy of mice. The Journal of biological chemistry. 2009a; 284:15173–15183. [PubMed: 19304658]

Maeda A, Maeda T, Golczak M, Palczewski K. Retinopathy in mice induced by disrupted all-trans-retinal clearance. The Journal of biological chemistry. 2008; 283:26684–26693. [PubMed: 18658157]

Maeda A, Maeda T, Imanishi Y, et al. Role of photoreceptor-specific retinol dehydrogenase in the retinoid cycle in vivo. The Journal of biological chemistry. 2005; 280:18822–18832. [PubMed: 15755727]

Maeda T, Cideciyan AV, Maeda A, Golczak M, Aleman TS, Jacobson SG, Palczewski K. Loss of cone photoreceptors caused by chromophore depletion is partially prevented by the artificial chromophore pro-drug, 9-cis-retinyl acetate. Human molecular genetics. 2009b; 18:2277–2287. [PubMed: 19339306]

Mata NL, Weng J, Travis GH. Biosynthesis of a major lipofuscin fluorophore in mice and humans with ABCR-mediated retinal and macular degeneration. Proceedings of the National Academy of Sciences of the United States of America. 2000; 97:7154–7159. [PubMed: 10852960]

Mears AJ, Kondo M, Swain PK, Takada Y, Bush RA, Saunders TL, Sieving PA, Swaroop A. Nrl is required for rod photoreceptor development. Nature genetics. 2001; 29:447–452. [PubMed: 11694879]

Michael R, Bron AJ. The ageing lens and cataract: a model of normal and pathological ageing. Philosophical transactions of the Royal Society of London. 2011; 366:1278–1292. [PubMed: 21402586]

Molday RS. ATP-binding cassette transporter ABCA4: Molecular properties and role in vision and macular degeneration. J Bioenerg Biomembr. 2007; 39:507–517. [PubMed: 17994272]

Molday RS, Zhang K. Defective lipid transport and biosynthesis in recessive and dominant Stargardt macular degeneration. Progress in lipid research. 2010; 49:476–492. [PubMed: 20633576]

Murdaugh LS, Avalle LB, Mandal S, Dill AE, Dillon J, Simon JD, Gaillard ER. Compositional studies of human RPE lipofuscin. J Mass Spectrom. 2010; 45:1139–1147. [PubMed: 20860013]

Mustafi D, Engel AH, Palczewski K. Structure of cone photoreceptors. Progress in retinal and eye research. 2009; 28:289–302. [PubMed: 19501669]

Mustafi D, Kevany BM, Genoud C, et al. Defective photoreceptor phagocytosis in a mouse model of enhanced S-cone syndrome causes progressive retinal degeneration. The FASEB journal : official publication of the Federation of American Societies for Experimental Biology. 2011; 25:3157–3176.

Nikonov SS, Daniele LL, Zhu X, Craft CM, Swaroop A, Pugh EN Jr. Photoreceptors of Nrl -/- mice coexpress functional S- and M-cone opsins having distinct inactivation mechanisms. The Journal of general physiology. 2005; 125:287–304. [PubMed: 15738050]

Owsley C, Jackson GR, White M, Feist R, Edwards D. Delays in rod-mediated dark adaptation in early age-related maculopathy. Ophthalmology. 2001; 108:1196–1202. [PubMed: 11425675]

Owsley C, McGwin G Jr, Jackson GR, Kallies K, Clark M. Cone- and rod-mediated dark adaptation impairment in age-related maculopathy. Ophthalmology. 2007; 114:1728–1735. [PubMed: 17822978]

Palczewska G, Maeda T, Imanishi Y, Sun W, Chen Y, Williams DR, Piston DW, Maeda A, Palczewski K. Noninvasive multiphoton fluorescence microscopy resolves retinol and retinal condensation products in mouse eyes. Nature medicine. 2010; 16:1444–1449.

Palczewski K. Focus on vision: 3 decades of remarkable contributions to biology and medicine. The FASEB journal : official publication of the Federation of American Societies for Experimental Biology. 2011; 25:439–443.

Patel N, Adewoyin T, Chong NV. Age-related macular degeneration: a perspective on genetic studies. Eye (London, England). 2008; 22:768–776.

Rattner A, Nathans J. Macular degeneration: recent advances and therapeutic opportunities. Nat Rev Neurosci. 2006; 7:860–872. [PubMed: 17033682]

Rotenstreich Y, Fishman GA, Anderson RJ. Visual acuity loss and clinical observations in a large series of patients with Stargardt disease. Ophthalmology. 2003; 110:1151–1158. [PubMed: 12799240]

Sakami S, Maeda T, Bereta G, et al. Probing mechanisms of photoreceptor degeneration in a new mouse model of the common form of autosomal dominant retinitis pigmentosa due to P23H opsin mutations. The Journal of biological chemistry. 2011; 286:10551–10567. [PubMed: 21224384]

Schmitz-Valckenberg S, Fleckenstein M, Helb HM, Charbel Issa P, Scholl HP, Holz FG. In vivo imaging of foveal sparing in geographic atrophy secondary to age-related macular degeneration. Investigative ophthalmology & visual science. 2009a; 50:3915–3921. [PubMed: 19339734]

Schmitz-Valckenberg S, Fleckenstein M, Scholl HP, Holz FG. Fundus autofluorescence and progression of age-related macular degeneration. Survey of ophthalmology. 2009b; 54:96–117. [PubMed: 19171212]

Schmitz-Valckenberg S, Holz FG, Bird AC, Spaide RF. Fundus autofluorescence imaging: review and perspectives. Retina (Philadelphia, Pa). 2008; 28:385–409.

Scilley K, Jackson GR, Cideciyan AV, Maguire MG, Jacobson SG, Owsley C. Early age-related maculopathy and self-reported visual difficulty in daily life. Ophthalmology. 2002; 109:1235–1242. [PubMed: 12093644]

Shelley EJ, Madigan MC, Natoli R, Penfold PL, Provis JM. Cone degeneration in aging and age-related macular degeneration. Archives of ophthalmology. 2009; 127:483–492. [PubMed: 19365029]

Shiose S, Chen Y, Okano K, et al. Toll-like receptor 3 is required for development of retinopathy caused by impaired all-trans-retinal clearance in mice. The Journal of biological chemistry. 2011; 286:15543–15555. [PubMed: 21383019]

Shroyer NF, Lewis RA, Yatsenko AN, Wensel TG, Lupski JR. Cosegregation and functional analysis of mutant ABCR (ABCA4) alleles in families that manifest both Stargardt disease and age-related macular degeneration. Human molecular genetics. 2001; 10:2671–2678. [PubMed: 11726554]

Soucy E, Wang Y, Nirenberg S, Nathans J, Meister M. A novel signaling pathway from rod photoreceptors to ganglion cells in mammalian retina. Neuron. 1998; 21:481–493. [PubMed: 9768836]

Sparrow JR. Bisretinoids of RPE lipofuscin: trigger for complement activation in age-related macular degeneration. Advances in experimental medicine and biology. 2010; 703:63–74. [PubMed: 20711707]

Tangelder GJ, Van der Heijde RG, Polak BC, Ringens PJ. Precision and reliability of retinal thickness measurements in foveal and extrafoveal areas of healthy and diabetic eyes. Investigative ophthalmology & visual science. 2008; 49:2627–2634. [PubMed: 18515592]

Thompson DA, Gal A. Vitamin A metabolism in the retinal pigment epithelium: genes, mutations, and diseases. Progress in retinal and eye research. 2003; 22:683–703. [PubMed: 12892646]

Tsybovsky Y, Molday RS, Palczewski K. The ATP-binding cassette transporter ABCA4: structural and functional properties and role in retinal disease. Advances in experimental medicine and biology. 2010; 703:105–125. [PubMed: 20711710]

Abbreviations used

ABCA4	ATP–binding cassette transporter 4
AF	autofluorescence
AMD	age–related macular degeneration
A2E	di–retinoid–pyridinium–ethanolamine

CRD	cone–rod dystrophy
DAPI	4,6–diamidino–2–phenylindole
DTA	cone–specific diphtheria toxin A
ERG	electroretinogram
GCL	ganglion cell layer
IHC	immunohistochemistry
INL	inner nuclear layer
IPL	inner plexiform layer
IS	inner segment(s)
LRAT	lecithin: retinol acyltransferase
MD	mean difference of sensitivity
Nrl	rod photoreceptor–specific neural retina leucine zipper protein
ONH	optic nerve head
ONL	outer nuclear layer
OS	outer segment(s)
PNA	peanut agglutinin
PSD	pattern standard deviation
RDH	retinol dehydrogenase
RP	retinitis pigmentosa
RPE	retinal pigmented epithelium
RPE65	retinal pigment epithelium–specific protein 65 kDa
SAP	standard automated perimetry
SLO	scanning laser ophthalmoscopy
SD–OCT	spectral domain–optical coherent tomography
STGD	Stargardt’s disease
WT	wild type

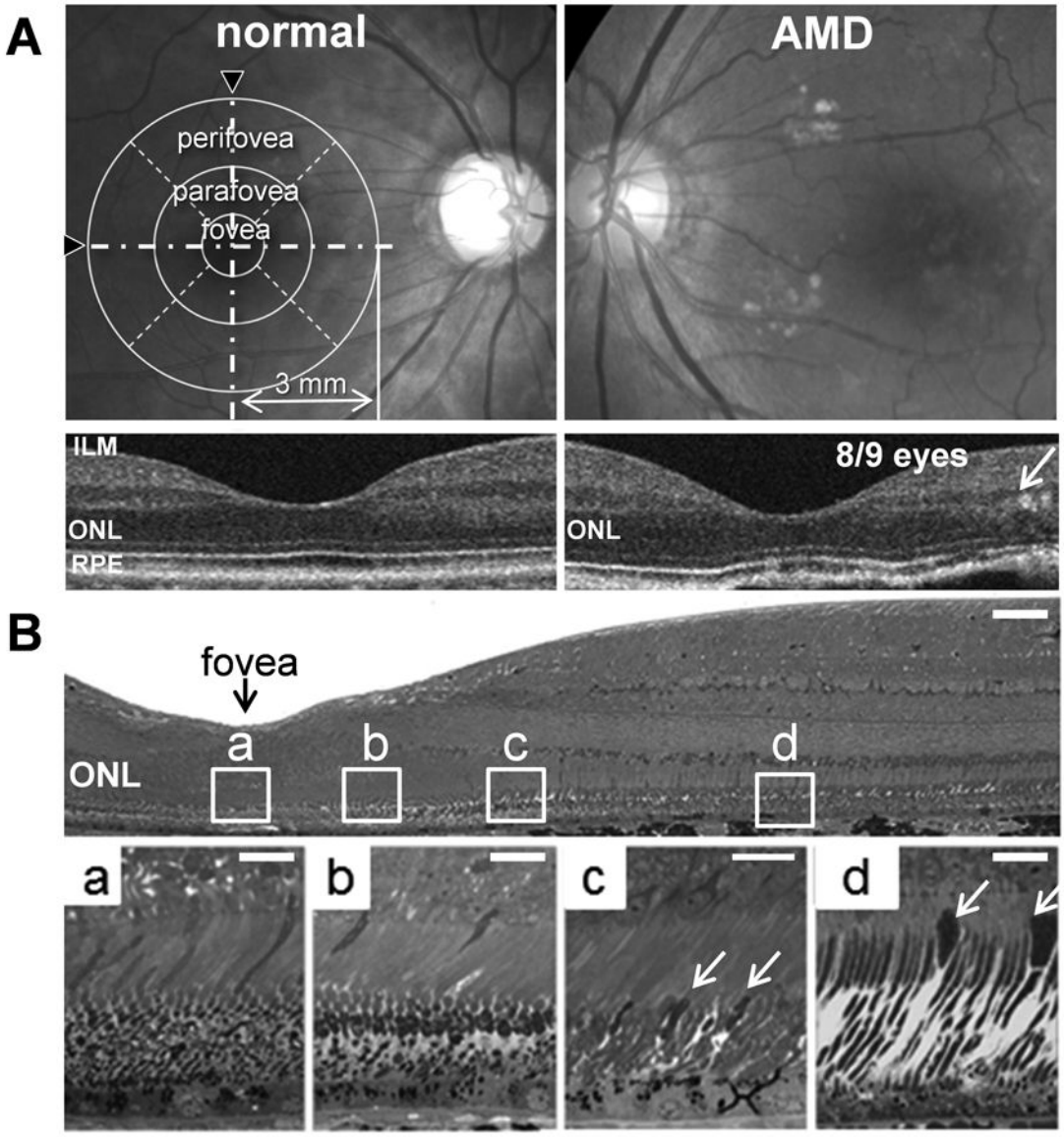

Figure 1. Photoreceptor topography in early age–related macular degeneration

Representative human fundus images from a healthy individual (normal) and a patient with early–stage AMD are shown (A upper). As indicated in the A upper left panel, the macular region was scanned within a 3 mm range of the central fovea. Retinal cross section images were obtained horizontally and vertically by crossing the foveal center in the B–scan mode (white dash–dot lines with black arrow heads in A upper left). Representative horizontal B–scan images also are shown (A lower). Retinal thickness of the foveal, parafoveal and perifoveal areas was evaluated by radial scanning of the macular region. The parafovea and perifovea were divided into 4 regions (white dashed–lines) and the thickness between inner limiting membranes (ILM) to RPE was averaged for each region. The thickness in each region was then compared with the distribution of thicknesses in the corresponding region exhibited by normal retinas. Regions exhibiting decreased thicknesses with a P value <5% as compared to normal were considered “decreased” and these are summarized in Table 1. Magnified horizontal B–scan images (A lower) with 2 mm range from the center of the macula (white arrow in A lower right) are shown. Eight of nine eyes from patients with early

stage AMD showed disruption of the ONL with pseudo–rosettes in the parafoveal or the perifoveal regions (Table 1). The B upper panel shows the macular region of an Epon–prepared macular region of a cynomolgus monkey and magnified images of 4 different lesions in the macula are presented in the B lower panels. The highest density of cones is present in the center of the macula (region a) and the density decreases in the region at 0.2 mm distance from the center (region b). The density of rods is markedly increased in the region 2.0 mm from the center (region c) and the more peripheral region (region d, 4.0 mm from the center) where the cone density (white arrows) is markedly decreased. The distribution in the region between “c” and “d” in B where cones and rods exist heterogeneously with a high rod/cone ratio corresponds to the pathological region noted in early stage AMD (A right panels). Bars in B upper panel, 40 μm; lower panels, 10 μm. ILM, inner limiting membrane; RPE, retinal pigmented epithelium; ONL, outer nuclear layer.

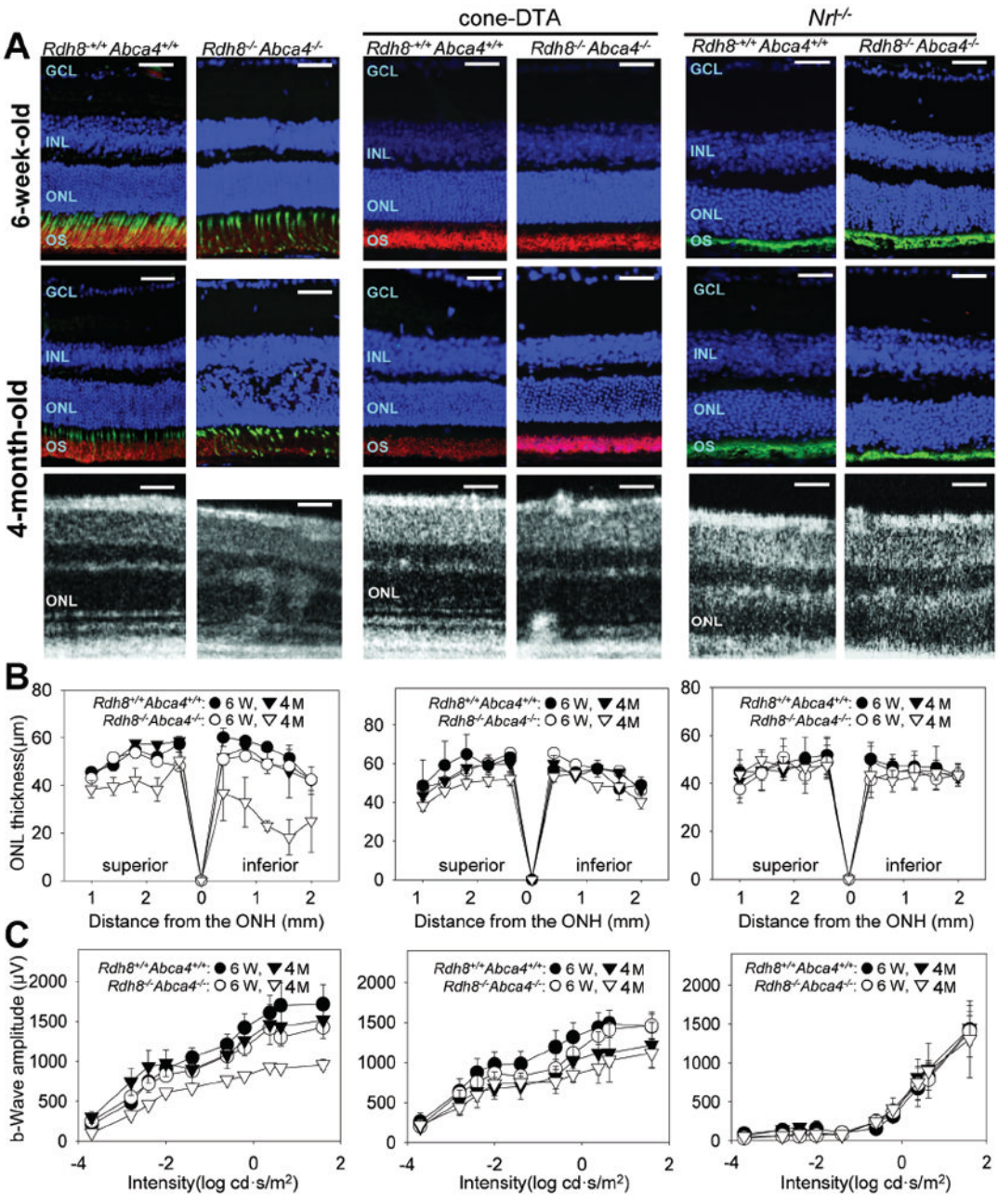

Figure 2. Cone–DTA *Rdh8*$^{-/-}$ *Abca4*$^{-/-}$ mice show earlier progression of photoreceptor cell death than *Nrl*$^{-/-}$ *Rdh8*$^{-/-}$ *Abca4*$^{-/-}$ mice, but *Rdh8*$^{-/-}$ *Abca4*$^{-/-}$ mice exhibit the earliest and most rapid progression of photoreceptor cell death

Progression of retinal degeneration in *Rdh8*$^{-/-}$ *Abca4*$^{-/-}$ (cone and rod), cone–DTA *Rdh8*$^{-/-}$ *Abca4*$^{-/-}$ (rod–only) and *Nrl*$^{-/-}$ *Rdh8*$^{-/-}$ *Abca4*$^{-/-}$ (cone–like–only) mice maintained under a 12 h light (~50 lux) /12 h dark cycle, was evaluated with IHC and SD–OCT imaging (A), measurements of ONL thickness in the superior and inferior retina (B), and scotopic single–flash ERG recordings (C). Cryo sections from 6–week–old and 4–month–old mice were stained with anti–rhodopsin antibody (1D4, red), and PNA (green) and DAPI (blue)(A top and middle panels). Mild photoreceptor cell death was observed in cone–DTA *Rdh8*$^{-/-}$ *Abca4*$^{-/-}$ mice whereas no significant changes in ONL thickness were

noted in *Nrl*$^{-/-}$ *Rdh8*$^{-/-}$ *Abca4*$^{-/-}$ mice at 4 months of age. However, *Rdh8*$^{-/-}$ *Abca4*$^{-/-}$ mice showed significant progression of degenerative changes with disruption of the OS and the ONL at 4 months of age. Similar pathological changes were observed in SD–OCT images obtained from each mouse model at 4 months of age (A bottom panels). Single flash ERG responses were recorded under scotopic conditions and functional b–wave amplitudes were plotted (C). Retinal dysfunction was observed in cone–DTA *Rdh8*$^{-/-}$ *Abca4*$^{-/-}$ mice and *Rdh8*$^{-/-}$ *Abca4*$^{-/-}$ mice that reflected their corresponding levels of retinal degeneration (C left and middle panels) whereas no significant dysfunction was recorded in *Nrl*$^{-/-}$ *Rdh8*$^{-/-}$ *Abca4*$^{-/-}$ mice (C right panels). Representative images of immunohistochemistry and SD-OCT were obtained in the inferior retina. GCL, ganglion cell layer; INL, inner nuclear layer; ONL, outer nuclear layer; PR, photoreceptor cells. Bars in A, 20 μm. Error bars indicate SDs in B and SEs in C ($n > 4$).

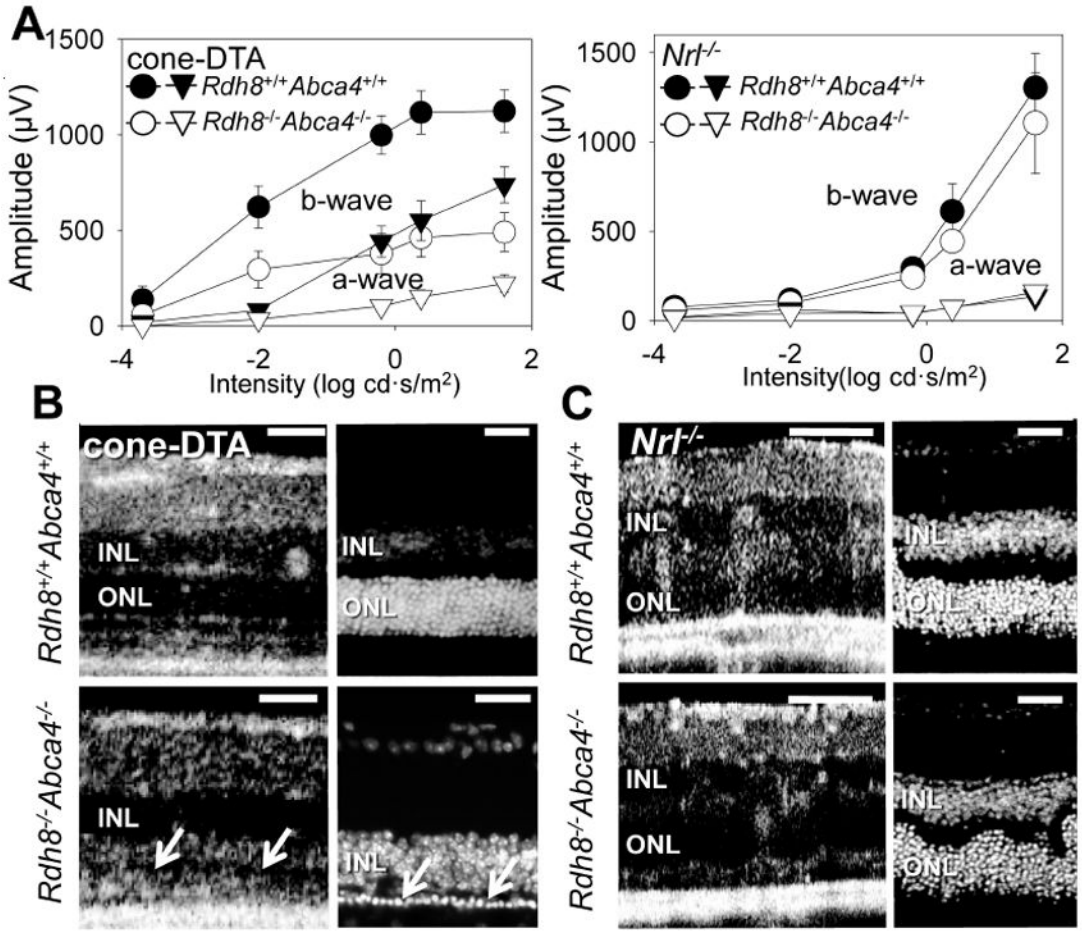

Figure 3. Rod cells are more susceptible to intense light–induced acute degeneration than cone cells

Six–week–old cone–DTA *Rdh8*$^{-/-}$ *Abca4*$^{-/-}$ and *Nrl*$^{-/-}$ *Rdh8*$^{-/-}$ *Abca4*$^{-/-}$ mice were exposed to intense light (10,000 lux) for 30 min to induce acute damage to the retina. Seven days after the light exposure, retinal function and morphology was evaluated by scotopic-ERG recordings and SD–OCT and IHC imaging with DAPI staining. ERG responses in cone-DTA*Rdh8*$^{-/-}$ *Abca4* $^{-/-}$ mice evidenced significant retinal dysfunction (>60% decreased response) whereas only mild dysfunction (<15% b–wave response depletion at high–intensity stimulation) was noted in *Nrl*$^{-/-}$ *Rdh8*$^{-/-}$ *Abca4*$^{-/-}$ mice. (A: filled symbols indicate mice without deletion of *Rdh8* and *Abca4*; unfilled symbols, *Rdh8*$^{-/-}$ *Abca4*$^{-/-}$; circles, b–waves; triangles, a–waves). Bars indicate SE of means (n > 3). Retinal morphological changes were examined with SD–OCT and IHC with DAPI staining in lesions at superior retina at 500 μm away from the optic nerve head center (B and C). Severe photoreceptor cell death was observed in cone–DTA *Rdh8*$^{-/-}$ *Abca4*$^{-/-}$ mice by SD–OCT (B left panel) as manifested by only 1or 2 rows of nuclei in the ONL (white arrows in B right panel). There was no significant morphological change in *Nrl*$^{-/-}$ *Rdh8*$^{-/-}$ *Abca4*$^{-/-}$ mice in SD–OCT (C left panel) and IHC images (C right panel). Error bars indicate SEs in A (*n* >3). Representative images of SD-OCT were obtained in the inferior retina. ONL, outer nuclear layer. Bars in B, C: 40 μm.

Table 1

Spectral domain optic coherence tomography (SD–OCT) imaging and Humphrey field analyzer (HFA) evaluation of early–stage AMD patients.

				SD–OCT				HFA	
				decrease in retinal thickness		ONL disruption with retinal folds			
Pt ID	Age (years)	Eye	VA[a]	fovea	para– or peri–fovea	fovea	para– or peri–fovea	MD (dB)	PSD (dB)
1	83	OD	20/20	+	−	−	Not clear	N.A.	N.A.
2	67	OD	20/20	−	+	−	+	0.12	1.79
		OS	20/20	−	+	−	+	0.3	1.35
3	72	OD	20/20	+	+	−	+	−3.16 (P<2%)	1.70 (P<5%)
4	75	OD	N.A.	−	+	−	+	N.A.	N.A.
		OS	N.A.	−	−	−	+	N.A.	N.A.
5	79	OS	20/20	−	−	−	+	−0.34	1.73
6	83	OD	N.A.	−	−	−	+	N.A.	N.A.
		OS	N.A.	−	+	−	+	N.A.	N.A.
Pathological changes in OCT				2/9 (22%)	5/9 (56%)	0/0 (0%)	8/9 (89%)		

[a]VA, visual acuity; MD, mean deviation; PSD, pattern standard deviation; N.A., not available; ONL, outer nuclear layer; dB, decibel.